PERGAMON

Annals of Nuclear Energy 28 (2001) 1563–1581

annals of
NUCLEAR ENERGY

www.elsevier.com/locate/anucene

On criticality calculations in multislab geometry

A.D. Caldeira [a], R.D.M. Garcia [a,b,*]

[a] *Centro Técnico Aeroespacial, Instituto de Estudos Avançados, 12231-970 São José dos Campos, SP, Brazil*

[b] *HSH Scientific Computing, Rua Carlos de Campos, 286, 12242-540 São José dos Campos, SP, Brazil*

Received 3 October 2000; accepted 14 October 2000

Abstract

The spherical-harmonics method is used to solve a class of multigroup criticality (k-eigenvalue) problems in multislab geometry. The model includes scattering anisotropy of arbitrary order and allows reflective or vacuum outer boundaries. Numerical results of benchmark quality are reported for three sample problems that have been defined and used by other authors to study various transport methods for criticality calculations. A comparison with our results indicates that some of the earlier results are in error.

1. Introduction

In a recent work (Caldeira and Garcia, 2001), we have used the spherical-harmonics (P_N) method to solve, in a spatially continuous way, the problem of an infinite array of plate-type fuel cells. Because the test case that was defined and used in that work involves a relatively large number of groups (64) and three material regions, a tabulation of the corresponding group constants would be too lengthy to report. Although we can provide these group constants by electronic means to anyone interested in solving our 64-group problem, we believe it useful, as an aid to researchers involved in code benchmarking, to report accurate numerical results for some criticality (k-eigenvalue) problems with fewer groups that have been defined in the literature. Since two of these problems involve vacuum outer boundaries, and our previous solution (Caldeira and Garcia, 2001) was developed for the specific case of reflective boundaries, we also report in this work the (slight) modifications needed in our approach to accommodate the case of a vacuum outer boundary.

*Corresponding author at HSH Scientific Computing. Tel.: +55-12-322-6217; fax: +55-12-344-1177.
E-mail address: rdmgarcia@uol.com.br (R.D.M. Garcia).

0306-4549/01/$ - see front matter
PII: S0306-4549(00)00119-5

With regard to the above-mentioned 64-group cell problem, we should add that Parsons (2000) has communicated discrete-ordinates results that confirm our P_{63} result (Caldeira and Garcia, 2001) for the effective multiplication factor k_{eff}. His best result ($k_{\text{eff}} = 1.2618$) was obtained using a Gauss–Legendre quadrature of order 128 and 20 mesh cells per region in the ONEDANT code (Alcouffe et al., 1997) and compares very well with our P_{63} result ($k_{\text{eff}} = 1.2617$).

2. Statement of the problem

We consider a system of R slabs (see Fig. 1) with a reflective boundary at $z_0 = 0$ and either a reflective or a vacuum boundary at z_R.

As in our previous work (Caldeira and Garcia, 2001), we can adapt the notation of Siewert (1993) to formulate our problem as the problem of solving, for $r = 1,2,\ldots, R$, the transport equation

$$\mu \frac{\partial}{\partial z} \mathbf{\Psi}_r(z, \mu) + \mathbf{S}_r \mathbf{\Psi}_r(z, \mu) = \frac{1}{2} \sum_{\ell=0}^{L} P_\ell(\mu) \mathbf{T}_{r,\ell} \int_{-1}^{1} P_\ell(\mu') \mathbf{\Psi}_r(z, \mu') \mathrm{d}\mu', \tag{1}$$

where

$$\mathbf{\Psi}_r(z, \mu) = \begin{pmatrix} \Psi_{r,1}(z, \mu) \\ \Psi_{r,2}(z, \mu) \\ \vdots \\ \Psi_{r,G}(z, \mu) \end{pmatrix} \tag{2}$$

is a G-vector with the group angular fluxes in region r as components, $z \in (z_{r-1}, z_r)$ is the space variable measured in cm, and $\mu \in [-1, 1]$ is the cosine of the polar angle that specifies the direction of neutron travel. In addition, $\mathbf{S}_r$ is a $G \times G$ diagonal matrix with the group total cross sections $s_{r,1}, s_{r,2}, \ldots, s_{r,G}$ in the diagonal and $\mathbf{T}_{r,\ell}$ is a $G \times G$ matrix with elements that are the ℓth Legendre moments of the neutron transfer cross sections, namely

$$\sigma_{ij}^r(\ell) = \sigma_{s,ij}^r(\ell) + (1/k) \chi_i^r \left(\nu\sigma_f\right)_j^r \delta_{\ell,0}, \quad 1 \leqslant i, j \leqslant G. \tag{3}$$

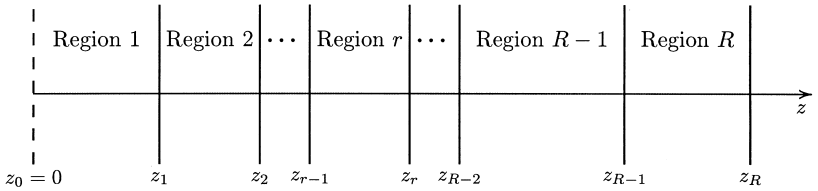

Fig. 1. Multislab geometry.

We note that in this expression $\sigma^r_{s,ij}(\ell)$ denotes the ℓth Legendre moment of the transfer cross section by scattering from group j to group i, k is a multiplication factor to be determined so that a physically meaningful solution of Eq. (1) exists in all regions, $\left(\nu\sigma_f\right)^r_j$ is the group j average of the number of neutrons emitted per fission times the fission cross section and χ^r_i is the fraction of fission neutrons that appear in group i. Here, we formulate our problem so that only the leftmost region ($r=1$) contains fissionable material. Thus, the second term on the right-hand side of Eq. (3) vanishes for $r=2,3,\ldots,R$. Moreover, the Kronecker delta in Eq. (3) indicates that we are considering the usual case of isotropic fission.

Now, to complete the formulation of our problem, we need to specify the boundary and interface conditions to which the group angular fluxes are subject. The reflective boundary condition at $z=z_0=0$ can be written, for $\mu \geqslant 0$, as

$$\mathbf{\Psi}_1(0,\mu) = \mathbf{\Psi}_1(0,-\mu), \tag{4a}$$

while at the interfaces z_r, $r=1,2,\ldots,R-1$, we consider the continuity conditions, for $\mu>0$,

$$\mathbf{\Psi}_r(z_r,\pm\mu) = \mathbf{\Psi}_{r+1}(z_r,\pm\mu), \tag{4b}$$

and the condition at the outer boundary of the system ($z=z_R$) can be written, for $\mu>0$, as

$$\mathbf{\Psi}_R(z_R,-\mu) = \rho\mathbf{\Psi}_R(z_R,\mu), \tag{4c}$$

where $\rho=1$ for a reflective boundary or $\rho=0$ for a vacuum boundary.

To close this section, we note that, instead of dealing directly with Eqs. (1) and (4), it is more convenient to deal with a version of these equations where the space variable is measured in terms of mean free paths (Siewert, 1993). For any region r, denoting as $s_{\min,r}$ the minimum of the group total cross sections in the region and introducing the dimensionless optical variable $\tau(z)=\tau_{r-1}+(z-z_{r-1})s_{\min,r}$, where

$$\tau_{r-1} = \sum_{i=1}^{r-1}(z_i - z_{i-1})s_{\min,i}, \tag{5}$$

we find that Eq. (1) can be rewritten, for $\tau\in(\tau_{r-1},\tau_r)$, as

$$\mu\frac{\partial}{\partial\tau}\mathbf{\Psi}_r(\tau,\mu) + \mathbf{\Sigma}_r\mathbf{\Psi}_r(\tau,\mu) = \frac{1}{2}\sum_{\ell=0}^{L}P_\ell(\mu)\mathbf{C}_{r,\ell}\int_{-1}^{1}P_\ell(\mu')\mathbf{\Psi}_r(\tau,\mu')\mathrm{d}\mu', \tag{6}$$

where $\mathbf{\Sigma}_r=\mathbf{S}_r/s_{\min,r}$ and $\mathbf{C}_{r,\ell}=\mathbf{T}_{r,\ell}/s_{\min,r}$. Similarly, we find that Eqs. (4) can be rewritten in terms of τ as

$$\mathbf{\Psi}_1(0,\mu) = \mathbf{\Psi}_1(0,-\mu), \quad \mu \geqslant 0, \tag{7a}$$

$$\mathbf{\Psi}_r(\tau_r, \pm\mu) = \mathbf{\Psi}_{r+1}(\tau_r, \pm\mu), \quad \mu > 0, \tag{7b}$$

for $r = 1, 2, \ldots, R-1$, and

$$\mathbf{\Psi}_R(\tau_R, -\mu) = \rho\mathbf{\Psi}_R(\tau_R, \mu), \quad \mu > 0. \tag{7c}$$

3. The P_N method for the case of a reflective outer boundary

As our application of the P_N method for the case $\rho = 1$ has been discussed in a recent work (Caldeira and Garcia, 2001), we only summarize here the main aspects of our solution for this case.

Beginning with the fuel region, we write the P_N solution that satisfies the first $N+1$ moments of Eq. (6) for $r=1$ and the reflective condition expressed by Eq. (7a) as

$$\mathbf{\Psi}_1(\tau,\mu) = \frac{1}{2}\sum_{n=0}^{N}(2n+1)\mathbf{\Phi}_{1,n}(\tau)P_n(\mu), \tag{8}$$

where

$$\begin{aligned}\mathbf{\Phi}_{1,n}(\tau) = {} & \sum_{j=1}^{J_I} A_{1,j}\mathbf{Z}^{-}_{1,n}(\tau,\xi_{1,j}) + \sum_{j=J_I+1}^{J_S} A_{1,j}\left[\mathrm{e}^{-(\tau_1+\tau)/\xi_{1,j}} + (-1)^n\mathrm{e}^{-(\tau_1-\tau)/\xi_{1,j}}\right]\mathbf{G}_{1,n}(\xi_{1,j}) \\ & + \sum_{\substack{j=J_S+1 \\ \Delta j=2}}^{J-1}\left\{A_{1,j}\left[\mathrm{e}^{-\lambda_{1,j}(\tau_1+\tau)/(\xi_{1,j}\bar{\xi}_{1,j})}\mathbf{Z}^{-}_{1,n}(\tau,\xi_{1,j}) + (-1)^n\mathrm{e}^{-\lambda_{1,j}(\tau_1-\tau)/(\xi_{1,j}\bar{\xi}_{1,j})}\mathbf{Z}^{+}_{1,n}(\tau,\xi_{1,j})\right]\right. \\ & \left. + A_{1,j+1}\left[\mathrm{e}^{-\lambda_{1,j}(\tau_1+\tau)/(\xi_{1,j}\bar{\xi}_{1,j})}\mathbf{W}^{+}_{1,n}(\tau,\xi_{1,j}) - (-1)^n\mathrm{e}^{-\lambda_{1,j}(\tau_1-\tau)/(\xi_{1,j}\bar{\xi}_{1,j})}\mathbf{W}^{-}_{1,n}(\tau,\xi_{1,j})\right]\right\}. \end{aligned} \tag{9}$$

To express $\mathbf{\Phi}_{1,n}(\tau)$, the nth Legendre moment of the angular flux vector in the fuel, as we did in Eq. (9), we have assumed that the P_N eigenvalues (Siewert and Thomas, 1987; Siewert, 1993; Caldeira and Garcia, 2001) in $\mathcal{H}^*$, the region of the complex plane defined by $\Re z > 0$ and the *positive* half of the y-axis, are ordered so that $\xi_{1,j} = i\eta_{1,j}$, $j = 1, 2, \ldots, J_I$, are pure imaginary numbers, $\xi_{1,j}$, $j = J_I+1, J_I+2, \ldots, J_S$, are real, and the pairs $(\xi_{1,j}, \bar{\xi}_{1,j})$, $j = J_S+1, J_S+3, \ldots, J-1$, with $\xi_{1,j} = \lambda_{1,j} + i\eta_{1,j}$, are complex conjugate. We note that the total number of P_N eigenvalues in $\mathcal{H}^*$ is $J = G(N+1)/2$ and that the restriction $\Delta j = 2$ attached to the third summation symbol on the right-hand side of Eq. (9) means that j is to be incremented by two in that summation. Still with regard to the third summation on the right-hand side of Eq. (9), we note that Garcia and Siewert (1986) were the first to point out the possibility of complex conjugate pairs of P_N eigenvalues that split off the continuum

$[-1, 1]$ in P_N solutions to vector transport problems. In addition, we have used in Eq. (9) the general definitions

$$\mathbf{Z}^{\pm}_{r,n}(\tau,\xi)=\cos\left[\eta\tau/\left(\xi\bar{\xi}\right)\right]\Re\{\mathbf{G}_{r,n}(\xi)\}\pm\sin\left[\eta\tau/\left(\xi\bar{\xi}\right)\right]\Im\{\mathbf{G}_{r,n}(\xi)\} \tag{10}$$

and

$$\mathbf{W}^{\pm}_{r,n}(\tau,\xi)=\sin\left[\eta\tau/\left(\xi\bar{\xi}\right)\right]\Re\{\mathbf{G}_{r,n}(\xi)\}\pm\cos\left[\eta\tau/\left(\xi\bar{\xi}\right)\right]\Im\{\mathbf{G}_{r,n}(\xi)\}, \tag{11}$$

where $\mathbf{G}_{r,n}(\xi)$ is a G-vector that satisfies, for region r, the recurrence relation

$$\xi\mathbf{h}_{r,\ell}\mathbf{G}_{r,\ell}(\xi)=(\ell+1)\mathbf{G}_{r,\ell+1}(\xi)+\ell\mathbf{G}_{r,\ell-1}(\xi),\quad \ell\geqslant 0, \tag{12}$$

with

$$\mathbf{h}_{r,\ell}=\begin{cases}(2\ell+1)\boldsymbol{\Sigma}_r-\mathbf{C}_{r,\ell}, & \ell\leqslant L,\\ (2\ell+1)\boldsymbol{\Sigma}_r, & \ell>L,\end{cases} \tag{13}$$

and the truncation condition $\mathbf{G}_{r,N+1}(\xi)=\mathbf{0}$, when $\xi=\xi_{r,j}$, $j=1,2,\ldots,J$. Moreover, the (real) coefficients $A_{1,j}$, $j=1,2,\ldots,J$, in Eq. (9) are yet to be determined.

Continuing, we write the P_N solution that satisfies the first $N+1$ moments of Eq. (6) for any intermediate region $(2\leqslant r\leqslant R-1)$ as

$$\boldsymbol{\Psi}_r(\tau,\mu)=\frac{1}{2}\sum_{n=0}^{N}(2n+1)\boldsymbol{\Phi}_{r,n}(\tau)P_n(\mu), \tag{14}$$

where

$$\begin{aligned}\boldsymbol{\Phi}_{r,n}(\tau)=&\sum_{j=1}^{J_R}\left[A_{r,j}\mathrm{e}^{-(\tau-\tau_{r-1})/\xi_{r,j}}+(-1)^nB_{r,j}\mathrm{e}^{-(\tau_r-\tau)/\xi_{r,j}}\right]\mathbf{G}_r\left(\xi_{r,j}\right)\\&+\sum_{\substack{j=J_R+1\\ \Delta j=2}}^{J-1}\left\{\left[A_{r,j}\mathbf{Z}^{-}_{r,n}\left(\tau-\tau_{r-1},\xi_{r,j}\right)+A_{r,j+1}\mathbf{W}^{+}_{r,n}\left(\tau-\tau_{r-1},\xi_{r,j}\right)\right]\mathrm{e}^{-\lambda_{r,j}(\tau-\tau_{r-1})/\left(\xi_{r,j}\bar{\xi}_{r,j}\right)}\right.\\&\left.+(-1)^n\left[B_{r,j}\mathbf{Z}^{-}_{r,n}\left(\tau_r-\tau,\xi_{r,j}\right)+B_{r,j+1}\mathbf{W}^{+}_{r,n}\left(\tau_r-\tau,\xi_{r,j}\right)\right]\mathrm{e}^{-\lambda_{r,j}(\tau_r-\tau)/\left(\xi_{r,j}\bar{\xi}_{r,j}\right)}\right\}.\end{aligned} \tag{15}$$

Again, we have assumed that the P_N eigenvalues are ordered so that $\xi_{r,j}$, $j=1,2,\ldots,J_R$, are real and $\left(\xi_{r,j},\bar{\xi}_{r,j}\right)$, $j=J_R+1,J_R+3,\ldots,J-1$, with $\xi_{r,j}=\lambda_{r,j}+i\eta_{r,j}$, are complex conjugate pairs. The (real) coefficients $A_{r,j}$ and $B_{r,j}$, $j=1,2,\ldots,J$, that appear in Eq. (15) are yet to be determined.

Finally, considering the outermost region $(r=R)$, we write the P_N solution that satisfies the first $N+1$ moments of Eq. (6) for $r=R$ and the reflective condition expressed by Eq. (7c) with $\rho=1$ as

$$\mathbf{\Psi}_R(\tau,\mu)=\frac{1}{2}\sum_{n=0}^{N}(2n+1)\mathbf{\Phi}_{R,n}(\tau)P_n(\mu), \tag{16}$$

where

$$\begin{aligned}\mathbf{\Phi}_{R,n}(\tau)=&\sum_{j=1}^{J_R}A_{R,j}\left[\mathrm{e}^{-(\tau-\tau_{R-1})/\xi_{R,j}}+(-1)^n\mathrm{e}^{-(2\tau_R-\tau_{R-1}-\tau)/\xi_{R,j}}\right]\mathbf{G}_{R,n}\left(\xi_{R,j}\right)\\&+\sum_{\substack{j=J_R+1\\ \Delta j=2}}^{J-1}\left\{\left[A_{R,j}\mathbf{Z}^{-}_{R,n}\left(\tau-\tau_{R-1},\xi_{R,j}\right)+A_{R,j+1}\mathbf{W}^{+}_{R,n}\left(\tau-\tau_{R-1},\xi_{R,j}\right)\right]\mathrm{e}^{-\lambda_{R,j}(\tau-\tau_{R-1})/\left(\xi_{R,j}\bar{\xi}_{R,j}\right)}\right.\\&+(-1)^n\left[A_{R,j}\mathbf{Z}^{-}_{R,n}\left(2\tau_R-\tau_{R-1}-\tau,\xi_{R,j}\right)+A_{R,j+1}\mathbf{W}^{+}_{R,n}\left(2\tau_R-\tau_{R-1}-\tau,\xi_{R,j}\right)\right]\\&\left.\times\,\mathrm{e}^{-\lambda_{R,j}(2\tau_R-\tau_{R-1}-\tau)/\left(\xi_{R,j}\bar{\xi}_{R,j}\right)}\right\}.\end{aligned} \tag{17}$$

As before, we have assumed that the P_N eigenvalues are ordered so that $\xi_{R,j}$, $j=1,2,\ldots,J_R$, are real and $\left(\xi_{R,j},\bar{\xi}_{R,j}\right)$, $j=J_R+1,J_R+3,\ldots,J-1$, with $\xi_{R,j}=\lambda_{R,j}+i\eta_{R,j}$, are complex conjugate pairs. The (real) coefficients $A_{R,j}$, $j=1,2,\ldots,J$, that appear in Eq. (17) are yet to be determined.

It is clear from the above presentation that we have a total of $2J(R-1)$ unknown coefficients in Eqs. (9), (15) and (17). We can generate the same number of equations by considering Mark versions of the interface conditions defined by Eq. (7b), i.e.

$$\mathbf{\Psi}_r\left(\tau_r,\pm\mu_m\right)=\mathbf{\Psi}_{r+1}\left(\tau_r,\pm\mu_m\right), \tag{18}$$

for $r=1,2,\ldots,R-1$ and $m=1,2,\ldots,(N+1)/2$, where μ_m denotes the mth element in the set of $(N+1)/2$ positive zeros of the Legendre polynomial $P_{N+1}(\mu)$. We thus obtain the homogeneous system of linear algebraic equations (Caldeira and Garcia, 2001)

$$\mathbf{MX}=\mathbf{0}, \tag{19}$$

where the matrix $\mathbf{M}$ is of the form

$$\mathbf{M}=\begin{pmatrix}\mathbf{C}&-\mathbf{U}_2&-\mathbf{V}_2&\mathbf{0}&\mathbf{0}&\mathbf{0}&\cdots&\mathbf{0}&\mathbf{0}\\ \mathbf{D}&\mathbf{R}_2&-\mathbf{S}_2&\mathbf{0}&\mathbf{0}&\mathbf{0}&\cdots&\mathbf{0}&\mathbf{0}\\ \mathbf{0}&\mathbf{V}_2&\mathbf{U}_2&-\mathbf{U}_3&-\mathbf{V}_3&\mathbf{0}&\cdots&\mathbf{0}&\mathbf{0}\\ \mathbf{0}&\mathbf{S}_2&-\mathbf{R}_2&-\mathbf{R}_3&\mathbf{S}_3&\mathbf{0}&\cdots&\mathbf{0}&\mathbf{0}\\ \vdots&\vdots&\ddots&\ddots&\ddots&\ddots&\ddots&\vdots&\vdots\\ \mathbf{0}&\mathbf{0}&\cdots&\mathbf{0}&\mathbf{V}_{R-2}&\mathbf{U}_{R-2}&-\mathbf{U}_{R-1}&-\mathbf{V}_{R-1}&\mathbf{0}\\ \mathbf{0}&\mathbf{0}&\cdots&\mathbf{0}&\mathbf{S}_{R-2}&-\mathbf{R}_{R-2}&-\mathbf{R}_{R-1}&\mathbf{S}_{R-1}&\mathbf{0}\\ \mathbf{0}&\mathbf{0}&\cdots&\mathbf{0}&\mathbf{0}&\mathbf{0}&\mathbf{V}_{R-1}&\mathbf{U}_{R-1}&-\mathbf{E}\\ \mathbf{0}&\mathbf{0}&\cdots&\mathbf{0}&\mathbf{0}&\mathbf{0}&\mathbf{S}_{R-1}&-\mathbf{R}_{R-1}&-\mathbf{F}\end{pmatrix} \tag{20}$$

and the vector $\mathbf{X}$ is defined as

$$\mathbf{X} = \begin{pmatrix} \mathbf{A}_1 \\ \mathbf{A}_2 \\ \mathbf{B}_2 \\ \mathbf{A}_3 \\ \vdots \\ \mathbf{B}_{R-2} \\ \mathbf{A}_{R-1} \\ \mathbf{B}_{R-1} \\ \mathbf{A}_R \end{pmatrix}. \tag{21}$$

As explicit expressions for the $J\times J$ submatrices $\mathbf{C}$, $\mathbf{D}$, $\mathbf{E}$, $\mathbf{F}$, and $\mathbf{U}_r$, $\mathbf{V}_r$, $\mathbf{R}_r$ and $\mathbf{S}_r$, $r=2, 3, \ldots, R-1$, that are used to define $\mathbf{M}$ in Eq. (20) have been given in Appendix A of Caldeira and Garcia (2001), we do not repeat their definitions here. The subvectors $\mathbf{A}_r$, $r=1, 2, \ldots, R$, and $\mathbf{B}_r$, $r = 2, 3, \ldots, R-1$, that appear on the right-hand side of Eq. (21) are all of dimension J and have as their jth components the unknown coefficients $A_{r,j}$, $r = 1, 2, \ldots, R$, and $B_{r,j}$, $r = 2, 3, \ldots, R-1$, respectively.

Now, since a homogeneous linear system has a nontrivial solution only if the determinant of the corresponding matrix of coefficients vanishes, $\det \mathbf{M} = 0$ turns out to be the critical condition that allows us to find k_{eff}, the (largest) value of k in Eq. (3) that gives rise to a physically meaningful solution of Eq. (1) in all regions. In addition, a vector $\mathbf{X} \neq \mathbf{0}$ in the null space of the critical matrix $\mathbf{M}$ yields a set of subvectors $\mathbf{A}_r$, $r=1, 2,\ldots, R$, and $\mathbf{B}_r$, $r=2, 3,\ldots, R-1$, that solve the homogeneous system defined by Eq. (19). Once these vectors are available, all of the coefficients in the P_N solutions become known, up to a normalization factor that can be freely chosen.

To close this section, we note that the first ($n=0$) and second ($n=1$) Legendre moments expressed by Eqs. (9), (15) and (17) are our P_N approximations to the scalar flux and current vectors in the fuel, intermediate and outermost regions, respectively.

4. Modifications for the case of a vacuum outer boundary

The modifications that are needed to handle the case $\rho=0$ in Eq. (7c) are very simple. First we note that the P_N solutions for the fuel and the intermediate regions have exactly the same form as those given for the case $\rho=1$ in Section 3. To treat the outermost region properly, we now take the P_N solution expressed by Eqs. (14) and (15) for the intermediate regions $r=2, 3,\ldots, R-1$ to be valid also for $r=R$ when $\rho=0$. Clearly, due to the presence of the coefficients $B_{R,j}$, $j=1, 2,\ldots, J$, in the P_N solution for the outermost region, the number of unknowns is now $2J(R-1/2)$, which represents an increase of J unknowns when compared to the case $\rho=1$. The extra number of equations required to match the number of equations to the number of unknowns comes from a Mark version of Eq. (7c) for $\rho=0$, namely

$$\mathbf{\Psi}_R(\tau_R, -\mu_m) = \mathbf{0} \tag{22}$$

for $m = 1, 2, \ldots, (N+1)/2$. It turns out that the homogeneous system of linear algebraic equations that gives rise to the critical condition has, in this case, size $2J(R-1/2)$ and can be expressed as

$$\mathbf{NY} = \mathbf{0}, \tag{23}$$

where the critical matrix $\mathbf{N}$ is defined as

$$\mathbf{N} = \begin{pmatrix}
\mathbf{C} & -\mathbf{U}_2 & -\mathbf{V}_2 & \mathbf{0} & \mathbf{0} & \mathbf{0} & \cdots & \mathbf{0} & \mathbf{0} & \mathbf{0} \\
\mathbf{D} & \mathbf{R}_2 & -\mathbf{S}_2 & \mathbf{0} & \mathbf{0} & \mathbf{0} & \cdots & \mathbf{0} & \mathbf{0} & \mathbf{0} \\
\mathbf{0} & \mathbf{V}_2 & \mathbf{U}_2 & -\mathbf{U}_3 & -\mathbf{V}_3 & \mathbf{0} & \cdots & \mathbf{0} & \mathbf{0} & \mathbf{0} \\
\mathbf{0} & \mathbf{S}_2 & -\mathbf{R}_2 & -\mathbf{R}_3 & \mathbf{S}_3 & \mathbf{0} & \cdots & \mathbf{0} & \mathbf{0} & \mathbf{0} \\
\vdots & \vdots & \ddots & \ddots & \ddots & \ddots & \ddots & \vdots & \vdots & \vdots \\
\mathbf{0} & \mathbf{0} & \cdots & \mathbf{0} & \mathbf{V}_{R-2} & \mathbf{U}_{R-2} & -\mathbf{U}_{R-1} & -\mathbf{V}_{R-1} & \mathbf{0} & \mathbf{0} \\
\mathbf{0} & \mathbf{0} & \cdots & \mathbf{0} & \mathbf{S}_{R-2} & -\mathbf{R}_{R-2} & -\mathbf{R}_{R-1} & \mathbf{S}_{R-1} & \mathbf{0} & \mathbf{0} \\
\mathbf{0} & \mathbf{0} & \cdots & \mathbf{0} & \mathbf{0} & \mathbf{0} & \mathbf{V}_{R-1} & \mathbf{U}_{R-1} & -\mathbf{U}_R & -\mathbf{V}_R \\
\mathbf{0} & \mathbf{0} & \cdots & \mathbf{0} & \mathbf{0} & \mathbf{0} & \mathbf{S}_{R-1} & -\mathbf{R}_{R-1} & -\mathbf{R}_R & \mathbf{S}_R \\
\mathbf{0} & \mathbf{0} & \cdots & \mathbf{0} & \mathbf{0} & \mathbf{0} & \mathbf{0} & \mathbf{0} & \mathbf{V}_R - \mathbf{S}_R & \mathbf{U}_R + \mathbf{R}_R
\end{pmatrix} \tag{24}$$

and the vector of unknowns $\mathbf{Y}$ as

$$\mathbf{Y} = \begin{pmatrix} \mathbf{X} \\ \mathbf{B}_R \end{pmatrix}, \tag{25}$$

with $\mathbf{X}$ being defined as in Eq. (21).

5. Computational implementation

As our computational implementation of the method has been discussed in detail in a previous work (Caldeira and Garcia, 2001) only a brief discussion is given here.

In our FORTRAN program, the k-eigenvalue search is done by bisection, with the lower and upper initial estimates of k_{eff} being obtained, for any N, by: (i) adding and subtracting a suitable Δk to an estimate, say k_0, of k_{eff} that can be obtained from a low order (e.g. P_1 or P_3) sweep search performed between arbitrarily chosen lower and upper limits of k, say k_{inf} and k_{sup}; (ii) computing the determinant of $\mathbf{M}$ or $\mathbf{N}$, depending on the case, for $k_1 = k_0 - \Delta k$ and $k_2 = k_0 + \Delta k$; and (iii) repeating, if necessary, the procedure with the value of Δk doubled as many times as required until a sign change in the determinants is observed. The values of k_1 and k_2 so obtained are the required lower and upper estimates of k_{eff}. The k-eigenvalue search is terminated when the search interval has been halved sufficiently many times by the bisection procedure so that the lower and upper extremes of the interval differ by less than a prescribed relative difference (10^{-8} was our choice in this work).

For each bisection (or sweep) step, the determinant of **M** or **N** is computed with the LINPACK subroutines DGECO and DGEDI (Dongarra et al., 1979). When the matrix being factored happens to be numerically close to singular, which is precisely the case here when the critical condition is satisfied, subroutine DGECO provides an approximate null vector that determines (up to a normalization constant) the unknown P_N coefficients. These coefficients can then be used to compute P_N approximations to the group scalar fluxes and currents.

Finally, as discussed in our previous work (Caldeira and Garcia, 2001) some special techniques were also required in this work for robustness of the algorithm. At each bisection (or sweep) step, after the P_N eigenvalues in the fuel region were computed they were ordered by increasing absolute values. In addition, the corresponding eigenvectors, which provide the required $\{\mathbf{G}_{1,n}(\xi_{r,j})\}$ in the fuel, were normalized to a Euclidean norm of unity and the sign of the component with largest absolute value in the first calculational step was preserved. In the absence of these normalization practices, we have observed that our computational procedure may fail because the pattern of signs displayed by the computed values of det **M** (or det **N**) as k is varied monotonically in a given interval may show a random behavior.

6. Numerical results

In this section, we apply our P_N solution reported in Sections 3 and 4 to three criticality problems that have been used as test cases by other authors.

6.1. Three-region, two-group problem with isotropic scattering

This problem was proposed by Häggblom et al. (1975) and was subsequently considered by Ackroyd et al. (1980) and Lee et al. (1985). It consists of two cases: control plate inserted and control plate withdrawn. In the case of control plate inserted, region 1 corresponds to the fuel, region 2 to the moderator (water) and region 3 to the control plate, and the coordinates that define the system boundaries and interfaces (see Fig. 1) are: $z_0 = 0$, $z_1 = 10$ cm, $z_2 = 11$ cm, and $z_3 = 11.5$ cm. Both boundaries are reflective in this problem. For the case with control plate withdrawn, there are only two regions (fuel and water), and the water region extends from $z_1 = 10$ cm to $z_2 = 11.5$ cm. The macroscopic cross-section set for this problem is given in Table 1, where we use the notation of Section 2. In passing, we note that the column labeled as Σ_a in Table 1 of Lee et al. (1985) should have been labeled as Σ_t.

In Table 2, we compare our P_N results for the effective multiplication factor with those of Lee et al. (1985) who also used the P_N method for solving this problem. It can be seen that the results are in excellent agreement for N up to 11, but not for $N = 15$. Looking at the way our results converge as N is increased further and having used the ANISN code (Engle, 1973) with a Gauss–Legendre quadrature of order 16 and 160 mesh points per region to obtain $k_{\text{eff}} = 0.32819$ and 0.56636, respectively for the cases with and without control plate, we have concluded that the P_{15} results of Lee et al. (1985) are in error.

On investigating the reason why the case with the control plate withdrawn requires a higher order of approximation to converge than the case with the control plate inserted, we have discovered an unusual feature of this transport problem. As shown in Table 3 for various orders of the approximation, the P_N eigenvalue in $\mathcal{H}^* = \{z|\Re z > 0\} \cup \{z|\Re z = 0 \vee \Im z > 0\}$ that approaches the discrete eigenvalue (Siewert and Thomas, 1987) in the fuel region as $N \to \infty$ is *imaginary* for the case with the

Table 1
Group cross sections (cm^{-1}) and fission spectrum for the three-region, two-group problem

Group constant	Fuel ($r=1$)	Water ($r=2$)	Control material ($r=3$)
$s_{r,1}$	0.3	0.401	0.8
$s_{r,2}$	1.0	1.3	2.0
$\sigma^r_{s,11}(0)$	0.27	0.32	0.6
$\sigma^r_{s,12}(0)$	0.0	0.0	0.0
$\sigma^r_{s,21}(0)$	0.01	0.08	0.0
$\sigma^r_{s,22}(0)$	0.9	1.29	0.1
$(\nu\sigma_f)^r_1$	0.0	0.0	0.0
$(\nu\sigma_f)^r_2$	0.12	0.0	0.0
χ^r_1	1.0	–	–
χ^r_2	0.0	–	–

Table 2
P_N results for the effective multiplication factor k_{eff}

	Control plate inserted		Control plate withdrawn	
N	This work	Lee et al. (1985)	This work	Lee et al. (1985)
1	0.320073	0.320073	0.578013	0.578013
3	0.327334	0.327334	0.569479	0.569480
5	0.328048	0.328048	0.567452	0.567452
7	0.328166	0.328166	0.566833	0.566833
9	0.328186	0.328186	0.566586	0.566586
11	0.328188	0.328188	0.566462	0.566462
15	0.328184	0.328244	0.566342	0.566106
99	0.328181	–	0.566193	–
199	0.328181	–	0.566190	–
299	0.328181	–	0.566189	–
399	0.328181	–	0.566189	–

Table 3
P_N approximations to the discrete eigenvalue in the fuel region

Case	$N=9$	$N=19$	$N=29$	$N=199$	$N=299$
Control plate inserted	i4.07867	i4.07850	i4.07847	i4.07847	i4.07847
Control plate withdrawn	3.51185	3.51409	3.51450	3.51481	3.51482

control plate inserted and *real* for the case with the control plate withdrawn, due to the difference in k_{eff}. These results are in agreement with the prescription for the number and nature of the discrete eigenvalues in two-group transport theory (Siewert and Shieh, 1967). The unusual feature here is the existence of a source-free transport problem (the case with the control plate withdrawn) which admits a stable solution asymptotically described by (real) exponential eigenmodes. We are not aware of a previous mention of this possibility in the literature.

A more physical explanation of this result can be formulated by comparing the results of infinite multiplication factor (k_∞) calculations for the fuel region and for the homogenized mixture of three (two, for the case with the control plate withdrawn) material regions. We note that methods for computing k_∞ for any number of groups are reported in Appendix B of Caldeira and Garcia (2001) and in Appendix A.V of Sood et al. (1999). The reason why it is important to pay attention to the k_∞ values is that the condition $k = k_\infty$ of the fuel determines the transition point from imaginary (plus possibly other real) discrete eigenvalues to real discrete eigenvalues only. More explicitly, when a system has k_{eff} smaller than the k_∞ for the fuel region, at least one discrete eigenvalue in the fuel must be imaginary, while for k_{eff} greater than the k_∞ for the fuel region, all discrete eigenvalues in the fuel must be real.

In this problem, we have $k_\infty = 0.4$ for the fuel region, which indicates that this region is in fact composed of a mixture of fuel and absorbing material. Moreover, for the homogenized mixture of fuel, water and control material we have $k_\infty = 0.229115$ and for the homogenized mixture of fuel and water $k_\infty = 0.617078$. Clearly, since for the case of control plate inserted k_{eff} is smaller than the k_∞ of the fuel, at least one discrete eigenvalue in the fuel must be imaginary in this case. On the other hand, k_{eff} is greater than the k_∞ of the fuel for the case of control plate withdrawn, and consequently no discrete eigenvalue in the fuel can be imaginary in this case. The question of how can such a system maintain a chain reaction can be answered by noting that k_{eff} is smaller than the k_∞ of the homogeneous mixture of fuel and water. Thus, it is the coupling between the source of fission neutrons produced in the fuel region and the source of thermalized neutrons sent back to the fuel by the water region that maintains the chain reaction in this case. This is clear from the behavior of the scalar fluxes depicted in Figs. 2 and 3 for the cases of control plate withdrawn and inserted, respectively. As shown in these figures, the group-2 (thermal) flux is strongly depressed near the outer boundary when the control plate is inserted, thus reducing the source of thermal neutrons that migrates to the fuel region and causes the peak of group-1 (fission) neutrons near the interface fuel/water that can be observed in Fig. 2.

In addition, a tabulation of the scalar fluxes and currents that can be used for benchmarking purposes is provided in Tables 4 and 5. The numerical results in these tables are thought to be accurate to within ± 1 in the last figure shown and were obtained, respectively, with $N = 599$ for Table 4 and $N = 499$ for Table 5. We note that all results for scalar fluxes and currents in this paper are normalised to a group-1 scalar flux of unity at $z = 0$.

Another interesting aspect of this problem is the conspicuosness of multiple values of the multiplication factor (k) associated with higher transport modes that satisfy

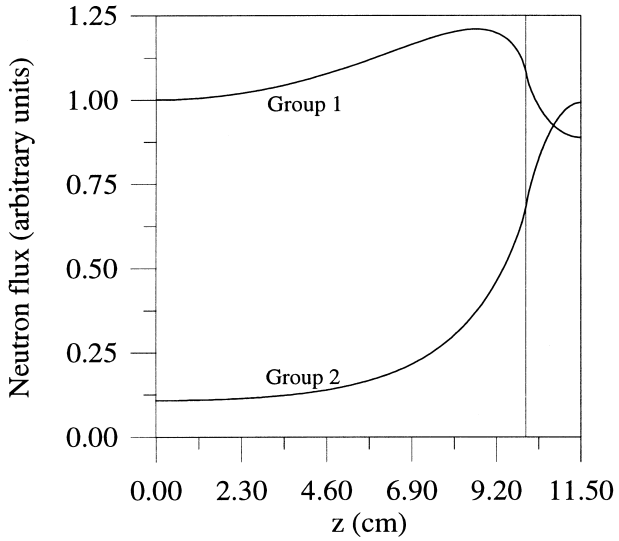

Fig. 2. The group scalar fluxes for the case of the control plate withdrawn.

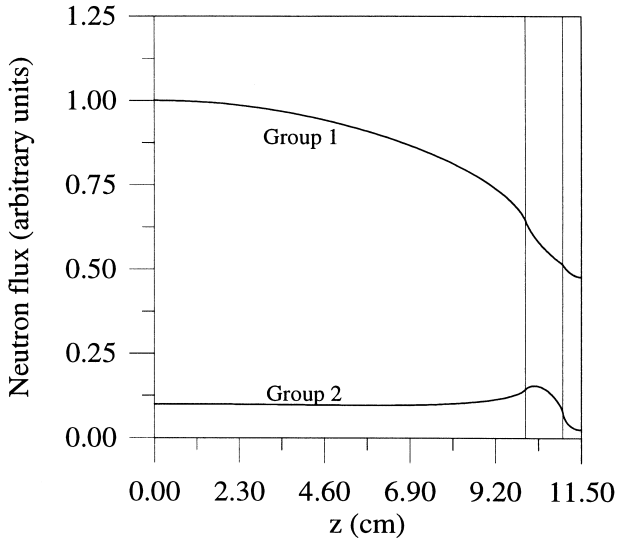

Fig. 3. The group scalar fluxes for the case of the control plate inserted.

the critical condition $\det \mathbf{M} = 0$. While most of these ks are clustered near zero and are very difficult to isolate, the first few can be easily computed with our code, using a sweep search in low order followed by specific bisection searches. In Table 6, we show, as a function of N, the largest four values of $k < k_{\text{eff}}$ that satisfy the critical condition for the case with the control plate withdrawn.

Table 4
The scalar fluxes and currents for the case with control plate inserted

Quantity	Group	$z=0$	$z=5$ cm	$z=10$ cm	$z=11$ cm	z = 11.5 cm
Scalar flux	1	1.00000(+0)	9.31582(−1)	6.46649(−1)	5.15035(−1)	4.77909(−1)
	2	9.87405(−2)	9.52501(−2)	1.42118(−1)	7.56614(−2)	2.34271(−2)
Current	1	0.00000(+0)	3.14339(−2)	9.50130(−2)	4.89735(−2)	0.00000(+0)
	2	0.00000(+0)	1.76579(−4)	−9.78293(−3)	3.43376(−2)	0.00000(+0)

Table 5
The scalar fluxes and currents for the case with control plate withdrawn

Quantity	Group	$z=0$	$z=5$ cm	$z=10$ cm	$z=11$ cm	$z=11.5$ cm
Scalar flux	1	1.00000(+0)	1.09151(+0)	1.08602(+0)	9.03593(−1)	8.87882(−1)
	2	1.07505(−1)	1.46743(−1)	6.80263(−1)	9.61243(−1)	9.91392(−1)
Current	1	0.00000(+0)	−2.87877(−2)	1.14449(−1)	3.61696(−2)	0.00000(+0)
	2	0.00000(+0)	−7.83109(−3)	−9.95971(−2)	−3.08162(−2)	0.00000(+0)

Table 6
P_N approximations to the largest four values of $k < k_{\text{eff}}$ for the case of control plate withdrawn

N	k_1	k_2	k_3	k_4
1	0.117343	0.0163965	0.00397183	0.00134503
3	0.127461	0.0237129	0.00721445	0.00288313
5	0.126927	0.0247128	0.00821962	0.00357324
7	0.126674	0.0248169	0.00849979	0.00385818
9	0.126569	0.0248174	0.00857458	0.00397002
19	0.126436	0.0247904	0.00859649	0.00403746
99	0.126393	0.0247783	0.00859149	0.00403551
199	0.126392	0.0247779	0.00859129	0.00403539
299	0.126391	0.0247778	0.00859125	0.00403537
399	0.126391	0.0247778	0.00859124	0.00403536

As expected from theoretical grounds (Davison, 1957; Bell and Glasstone, 1970; Duderstadt and Martin, 1979), we have confirmed numerically that none of these ks is associated with a neutron flux which is positive everywhere in the system, and so the only value of k relevant for this problem, physically speaking, is in fact $k_0 = k_{\text{eff}}$, as reported in Table 2.

6.2. *Two-region, 10-group problem with isotropic scattering*

This 10-group problem has been recently proposed by Batistela et al. (1999) in an application of a Laplace-transformed version of the discrete-ordinates method to

criticality calculations in plane geometry. The problem can be formulated as a two-region slab composed of fissionable material from $z=0$ to $z=7.5$ cm and nonfissionable material from $z=7.5$ cm to $z=27.5$ cm, where the inner boundary ($z=0$) is reflective and the outer one ($z=27.5$ cm) is a vacuum boundary.

The 10-group macroscopic cross sections and fission spectrum for this problem are defined in the work of Batistela et al. (1999) and are reproduced here in Tables 7–9. We note that we have detected an inconsistency in this data set, namely that the group-1 scattering cross section for region 2, obtained by summing up the scattering transfer cross sections given in the first row of Table 9, exceeds the corresponding total cross section ($s_{2,1}=0.691908$ cm^{-1}; see Table 7) by an amount of 0.007322 cm^{-1}.

In Table 10, we compare, in low order ($N\leqslant 9$), our k_{eff} results for this problem with the LTS_{N+1} results reported by Batistela et al. (1999) and the S_{N+1} results of Parsons (2000), who used the ONEDANT code (Alcouffe et al., 1997) with 5500 mesh cells and Gauss–Legendre quadrature. Due to the well-known equivalence (see, for example, the recent work by Barichello and Siewert, 1998) between the spherical-harmonics (P_N) method with Mark boundary conditions used in this

Table 7
The group constants $s_{r,i}$ and $\left(\nu\sigma_f\right)_i^1$ (in cm^{-1}) and the fission spectrum χ_i^1 for the 10-group problem

i	$s_{1,i}$	$s_{2,i}$	$\left(\nu\sigma_f\right)_i^1$	χ_i^1
1	0.2245876	0.691908	0.0009735	0.07
2	0.5529316	1.163784	0.001153	0.12
3	0.835548	1.146798	0.01756	0.202
4	1.4625101	1.281052	0.238	0.603
5	0.12507	0.35936	0.00081	0.0017
6	0.26377	0.2932	0.0035	0.001
7	0.644427	0.52023	0.0123	0.0006
8	0.8241506	0.71652	0.024	0.0004
9	0.28768	0.43845	0.005	0.0013
10	0.197631	0.07911	0.0009	0.0

Table 8
The scattering transfer cross sections $\sigma_{s,ij}^r$ (0) (in cm^{-1}) for region $r=1$ of the 10-group problem

j	$i=j-1$	$i=j$	$i=j+1$	$i=j+2$	$i=j+3$	$i=j+4$
1	0.0	0.16094	0.05824	0.003059	0.00123	0.00042
2	0.0325	0.45088	0.066442	0.00235	0.0	0.0
3	0.1234	0.63597	0.057518	0.0021	0.001	0.0
4	0.0006101	1.2839	0.0021	0.0003	0.0	0.0
5	0.001	0.07421	0.02176	0.0045	0.0021	0.0
6	0.0198	0.2019	0.02857	0.0104	0.0	0.0
7	0.1743	0.3689	0.046377	0.0444	0.01	0.0
8	0.0004426	0.30826	0.007038	0.5011	0.0	0.0
9	0.0938	0.1271	0.04561	0.0	0.0	0.0
10	0.000201	0.19296	0.0	0.0	0.0	0.0

Table 9
The scattering transfer cross sections $\sigma^r_{s,ij}(0)$ (in cm^{-1}) for region $r=2$ of the 10-group problem

j	$i=j-1$	$i=j$	$i=j+1$	$i=j+2$	$i=j+3$	$i=j+4$
1	0.0	0.24413	0.1741	0.051	0.2	0.03
2	0.174	0.62077	0.224	0.105	0.04	0.0
3	0.043	0.83158	0.152	0.09	0.03	0.0
4	0.074	1.1125	0.09	0.001	0.0	0.0
5	0.084	0.19286	0.0484	0.01	0.0	0.0
6	0.075	0.11588	0.0751	0.02	0.0	0.0
7	0.024	0.3571	0.123	0.007	0.0	0.0
8	0.077	0.4542	0.179	0.005	0.0	0.0
9	0.065	0.2742	0.0987	0.0	0.0	0.0
10	0.0004	0.07421	0.0	0.0	0.0	0.0

Table 10
Low-order results for the effective multiplication factor for the 10-group problem

N	P_N (this work)	LTS_{N+1} (Batistela et al., 1999)	S_{N+1} (Parsons, 2000)
1	1.09206	1.09206	1.09206
3	1.09615	1.09615	1.09615
5	1.09637	1.09637	1.09637
7	1.09643	1.09651	1.09643
9	1.09646	–	1.09646

work and the discrete-ordinates method with Gauss–Legendre points used by Batistela et al. (1999), perfect agreement between these numerical results was expected. However, as can be seen in Table 10, the P_N and LTS_{N+1} results are in complete agreement only for N up to 5. On the other hand, since an extremely fine grid was used in the ONEDANT calculations, the effects of spatial discretization on the results of this code were virtually eliminated and the agreement with the P_N results is perfect for all orders of the approximation. This led us to conclude that the LTS_8 result of Batistela et al. (1999) is not correct.

To provide even more accurate results for this problem, we report in Table 11 additional k_{eff} results that were obtained using our P_N code in high-order, along with the corresponding ONEDANT results of Parsons (2000), which are based on 22,000 mesh cells and either Gauss–Legendre (S_{N+1}) or double Gauss–Legendre (DS_{N+1}) quadratures. It can be seen that the double-Gauss results are the best of all, with the DS_{20} result being already correct in all figures shown. This is due to the much improved representation that can be achieved with the double Gauss–Legendre quadrature of the angular flux discontinuities that occur at interfaces and boundaries as $\mu \to 0$ from above and from below. In addition, P_{499} results for the scalar fluxes and currents, thought to be accurate to at least 5 significant figures, are given in Table 12.

Table 11
High-order results for the effective multiplication factor for the 10-group problem

N	P_N (this work)	S_{N+1} (Parsons, 2000)	DS_{N+1} (Parsons, 2000)
19	1.0964924	1.0964924	1.0965042
39	1.0965012	1.0965012	1.0965042
99	1.0965037	1.0965037	1.0965042
199	1.0965040	1.0965040	1.0965042
299	1.0965041	1.0965041	1.0965042
499	1.0965041	1.0965041	1.0965042

Table 12
The scalar fluxes and currents for the 10-group problem

	Scalar fluxes			Currents	
Group	$z=0$	$z=7.5$ cm	$z=27.5$ cm	$z=7.5$ cm	$z=27.5$ cm
1	1.00000(+0)	4.86623(−1)	3.50420(−5)	1.54279(−1)	2.09469(−5)
2	1.95428(+0)	7.23729(−1)	6.51246(−5)	2.20915(−1)	3.75497(−5)
3	9.90102(−1)	6.18599(−1)	7.09073(−4)	2.29819(−2)	4.09466(−4)
4	1.50456(+0)	1.21355(+0)	2.74287(−3)	2.08560(−3)	1.55963(−3)
5	4.05535(−1)	5.93068(−1)	7.86290(−3)	−8.84109(−2)	4.83488(−3)
6	2.80317(−1)	2.79649(−1)	4.81444(−3)	1.72825(−2)	2.99945(−3)
7	3.75173(−2)	1.05173(−1)	4.07103(−3)	−2.28986(−2)	2.36991(−3)
8	1.49238(−2)	5.61623(−2)	2.88601(−3)	−1.40445(−2)	1.65083(−3)
9	2.07038(−2)	5.56808(−2)	4.88800(−3)	−1.37163(−2)	2.87505(−3)
10	8.86504(−1)	8.11701(−1)	2.17840(−1)	6.28266(−2)	1.24471(−1)

6.3. Single-region, two-group problem with linearly anisotropic scattering

Originally, this two-group problem was formulated as a search of the critical half-thickness for a bare homogenous slab with linearly anisotropic scattering (Bosler, 1972; Bosler and Metcalf, 1972). In this work, we use a k-eigenvalue search to find the critical half-thickness z_1 that corresponds to $k_{\text{eff}}=1$. Two cases are considered: Case 1 corresponds to a mixture of 93% enriched uranium fuel and H_2O moderator and Case 2 to a mixture of uranium fuel and D_2O moderator. The corresponding macroscopic cross sections are given in a recent work (Sood et al., 1999) that includes a compilation of 75 problems intended for criticality code verification and are also given here in Table 13.

A slight variation of the second case, where $\left(\nu\sigma_f\right)_2=0.007043$ cm^{-1}, was considered by Ishiguro (1973) and is referred to as Case 3 in this work. In addition, we note that, contrary to the convention used to define the group structure for the first problem, the group numbers for this problem increase with increasing energies. We also note that the critical condition expressed by Eqs. (23)–(25) cannot be applied to a single-region problem, and, therefore, we have worked out a special formula for

this case. Using the notation introduced in Section 3, we find that the critical condition for a single-region problem can be written as

$$[\mathbf{C} + \mathbf{D}]\mathbf{A}_1 = \mathbf{0}, \tag{26}$$

where **C** and **D** are the $J \times J$ matrices defined in Appendix A of Caldeira and Garcia (2001).

In Table 14, we report our converged P_N results for the critical half-thicknesses for all three cases, thought to be accurate to within ± 1 in the last figure shown and obtained using $N = 299$ for Case 1 and $N = 19$ for Cases 2 and 3. In the same table, we show the numerical results of Bosler (1972) (see also Sood et al., 1999) and those of Ishiguro (1973). Both of these authors have used Case's method to solve this problem. On observing that our converged result for Case 1 agrees with that of Ishiguro, we conclude that only the first three figures of Bosler's result are correct for this case. We can also see that our result for Case 2 shows much better agreement with the corresponding result of Bosler and that our result for Case 3 agrees with Ishiguro's result. In addition, we note that our converged P_N results for Cases 1 and 2 have been independently confirmed by Parsons (2000), using the ONEDANT code.

Table 13
Group cross sections (cm^{-1}) and fission spectrum for the single-region, two-group problem

Group constant	Case 1	Case 2
s_1	2.52025	0.54628
s_2	0.65696	0.33588
$\sigma_{s,11}(0)$	2.44383	0.42410
$\sigma_{s,12}(0)$	0.029227	0.004555
$\sigma_{s,21}(0)$	0.0	0.0
$\sigma_{s,22}(0)$	0.62568	0.31980
$\sigma_{s,11}(1)$	2.49954	0.16317
$\sigma_{s,12}(1)$	0.0227211	−0.0011916
$\sigma_{s,21}(1)$	0.0	0.0
$\sigma_{s,22}(1)$	0.82377	0.20082
$(\nu\sigma_f)_1$	0.12658	0.24250
$(\nu\sigma_f)_2$	0.002621	0.0070425
χ_1	0.0	0.0
χ_2	1.0	1.0

Table 14
Critical half-thickness (cm) for the single-region, two-group problem

Case	Material	This work	Bosler (1972)	Ishiguro (1973)
1	$U + H_2O$	9.49590	9.491600	9.4959
2	$U + D_2O$	1000.54	1000.506133	–
3	$U + D_2O$	929.453	–	929.45

Table 15
The scalar fluxes and currents for Case 1

Quantity	Group	$z/z_1 = 0$	$z/z_1 = 0.2$	$z/z_1 = 0.5$	$z/z_1 = 0.8$	$z/z_1 = 1.0$
Scalar flux	1	1.00000(+0)	9.63273(−1)	7.75037(−1)	4.33839(−1)	7.67013(−2)
	2	2.76014(+0)	2.66033(+0)	2.15621(+0)	1.30377(+0)	5.22735(−1)
Current	1	0.00000(+0)	8.00148(−3)	1.92703(−2)	3.08691(−2)	4.38133(−2)
	2	0.00000(+0)	8.90345(−2)	2.07755(−1)	2.87253(−1)	3.01388(−1)

Table 16
The scalar fluxes and currents for Case 2

Quantity	Group	$z/z_1 = 0$	$z/z_1 = 0.2$	$z/z_1 = 0.5$	$z/z_1 = 0.8$	$z/z_1 = 1.0$
Scalar flux	1	1.00000(+0)	9.51306(−1)	7.08534(−1)	3.12090(−1)	2.35203(−3)
	2	2.68236(+1)	2.55175(+1)	1.90055(+1)	8.37140(+0)	8.90130(−2)
Current	1	0.00000(+0)	3.14139(−4)	7.19162(−4)	9.68208(−4)	1.32537(−3)
	2	0.00000(+0)	1.60474(−2)	3.67375(−2)	4.94597(−2)	5.14516(−2)

Closing this section, Tables 15 and 16 display our P_N results for the scalar fluxes and currents, obtained with $N = 699$ for Case 1 and $N = 899$ for Case 2. Since these numbers have not changed as we kept increasing the order of the approximation up to $N = 1499$ for both cases, we believe they are accurate in all figures shown.

7. Concluding remarks

In this work, we have used the P_N method to report especially accurate numerical results for three criticality problems in multislab geometry that have been used by other authors in previous studies. As discussed in detail in Section 6, existing tabulations in some works that intended to solve these problems accurately display errors, precluding the use of the numerical results in these tables as computational benchmarks.

Moreover, two of these problems revealed some features that we believe to be noteworthy. First, we mention the unusual case of a criticality problem that displays no imaginary discrete eigenvalue in the fuel region (viz. the case with control plate withdrawn studied in Subsection 6.1) and, second, the extreme sensitivity of the critical half-thickness for Case 2 of Subsection 6.3 to small changes in cross sections.

Acknowledgements

The authors would like to thank R.A. Forster, N.J. McCormick, D.K. Parsons and C.E. Siewert for helpful discussions. They are indebted to D.K. Parsons of Los Alamos National Laboratory for the numerical results generated with the ONEDANT

code, and to A. Passaro, coordinator of the Virtual Engineering Laboratory at CTA/IEAv, for computational resources that were used to perform some of the high-order P_N calculations. The work of R.D.M.G. was supported in part by CNPq.

References

Ackroyd, R.T., Ziver, A.K., Goddard, A.J.H., 1980. A finite element method for neutron transport. Part IV: a comparison of some finite element solutions of two group benchmark problems with conventional solutions. Ann. Nucl. Energy 7, 335–349.

Alcouffe, R.E., Baker, R.S., Brinkley, F.W., Marr, D.R., O'Dell, R.D., Walters, W.F., 1997. DANTSYS: A Diffusion Accelerated Neutral Particle Transport Code System. Report LA-12969-M (revised). Los Alamos National Laboratory, Los Alamos, NM.

Barichello, L.B., Siewert, C.E., 1998. On the equivalence between the discrete ordinates and the spherical harmonics methods in radiative transfer. Nucl. Sci. Eng. 130, 79–84.

Batistela, C.H.F., de Vilhena, M.T., Borges, V., 1999. Determination of the effective multiplication factor in a slab by the LTS_N method. Ann. Nucl. Energy 26, 761–767.

Bell, G.I., Glasstone, S., 1970. Nuclear Reactor Theory. Van Nostrand Reinhold, New York.

Bosler, G. E. 1972. Critical Slab Solution to the Two-Group Neutron Transport Equation for Linearly Anisotropic Scattering. PhD dissertation, University of Virginia.

Bosler, G.E., Metcalf, D.R., 1972. Critical slab solution to the two-group neutron transport equation for linearly anisotropic scattering. Trans. Am. Nucl. Soc. 15, 913–914.

Caldeira, A.D., Garcia, R.D.M., 2001. The P_N method for cell calculations of plate-type fuel assemblies. Transp. Theory Stat. Phys. (to appear)

Davison, B., 1957. Neutron Transport Theory. Oxford University Press, London.

Dongarra, J.J., Bunch, J.R., Moler, C.B., Stewart G.W., 1979. LINPACK Users' Guide. SIAM, Philadelphia, PA.

Duderstadt, J.J., Martin, W.R., 1979. Transport Theory. Wiley-Interscience, New York.

Engle Jr., W.W., 1973. A Users Manual for ANISN, a One Dimensional Discrete Ordinates Transport Code with Anisotropic Scattering. Report K-1693 (updated). Union Carbide, Nuclear Division, Oak Ridge, TN.

Garcia, R.D.M., Siewert, C.E., 1986. A generalized spherical harmonics solution for radiative transfer models that include polarization effects. J. Quant. Spectrosc. Radiat. Transfer 36, 401–423.

Häggblom, H., Ahlin, Å., Nakamura, T., 1975. Transmission probability method of integral neutron transport calculation for two-dimensional rectangular cells. Nucl. Sci. Eng. 56, 411–433.

Ishiguro, Y., 1973. Two-Group Neutron-Transport Theory with Linearly Anisotropic Scattering: Half-Range Orthogonality and Critical Slab Problem. Publication IEA No. 306. Instituto de Pesquisas Energéticas e Nucleares, São Paulo, SP, Brazil.

Lee, C.E., Fan, W.C.P., Dias, M.P, 1985. Analytical solutions to the moment transport equations — II: multiregion, multigroup 1-D slab, cylinder, and sphere criticality and source problems. Ann. Nucl. Energy 12, 613–632.

Parsons, D.K., 2000. Private communication.

Siewert, C.E., 1993. A spherical-harmonics method for multi-group or non-gray radiation transport. J. Quant. Spectrosc. Radiat. Transfer 49, 95–106.

Siewert, C.E., Shieh, P.S., 1967. Two-group transport theory. J. Nucl. Energy 21, 383–392.

Siewert, C.E., Thomas Jr., J.R., 1987. A method for computing the discrete spectrum basic to multi-group transport theory. J. Quant. Spectrosc. Radiat. Transfer 37, 111–115.

Sood, A., Forster, R.A., Parsons, D.K. 1999. Analytical Benchmark Test Set for Criticality Code Verification. Report LA-13511. Los Alamos National Laboratory, Los Alamos, NM.